Colour control of titanium nitride coatings produced by reactive magnetron sputtering at temperature less than 100°C

Roquiny, Philippe; Bodart, Franz; Terwagne, Guy

Published in:
Surface and Coatings Technology

Publication date:
1999

Document Version
Publisher's PDF, also known as Version of record

ELSEVIER

Surface and Coatings Technology 116–119 (1999) 278–283

SURFACE & COATINGS TECHNOLOGY

www.elsevier.nl/locate/surfcoat

Colour control of titanium nitride coatings produced by reactive magnetron sputtering at temperature less than 100°C

Ph. Roquiny *, F. Bodart, G. Terwagne

Laboratoire d'Analyses par Reactions Nucleaires, Facultés Universitaires Notre-Dame de la Paix, rue de Bruxelles 61, B-5000 Namur, Belgium

Abstract

Decorative dry coatings are extensively used nowadays to replace the current pollutant wet coating processes, but the links between the coating appearance and the physical properties are usually not fully understood. This paper presents the results obtained by optical measurements in order to investigate the import of titanium nitride physical properties such as stoichiometry and structure on the coating visual appearance for TiN_x thin films deposited by DC reactive magnetron sputtering at temperature lower than 100°C onto grounded substrate. It was shown that colours going from metallic grey to gold and finally brownish red have been obtained when the N_2 flow is raised. These TiN_x layer colour variations can be resolved in terms of the Drude model. As titanium metallic bonds decrease in the film, the absorbed part of the spectra moves towards lower energies, and when the minimum titanium content in the deposited films is reached (N_2 mass flow > 4 sccm), defects also reduce the amortised spectra towards slightly more reddish energies, but are difficult to control. In conclusion, as the N_2 content in the gas discharge guides the nitrogen composition, it is the key parameter in colour control for TiN_x sputtered films, especially when N_2 mass flow is less than 4 sccm.

Keywords: Colour; Magnetron sputtering; PVD; Thin film; TiN_x

1. Introduction

Wet coating processes now require more and more post-treating for the pollutant by-products as the environmental statutes and regulations become more restrictive. Then, the cost of wet coating technologies increases as the released by-product norms decrease. Both US and ECC environmental protection laws [1,2] condemn the material surface finishers to study new and clean deposition alternatives. Vapour deposition turns out to be competitive as a result of water and liquid-metal bath recycling cost and hazardous solvent banishment from the wet coating processes. Furthermore, physical and chemical vapour depositions (PVD and CVD) offer a large variety of material coatings, high experimental flexibility as well as the minimisation of waste disposal [3,4].

Among these waste-free surface processes, reactive magnetron sputtering of nitrides and carbides seems to offer a great deal of interest in decorative application for large area substrates [4–8]. For example, the transition metal nitrides combine attractive colours with superior wear resistance, good adhesion and chemical stability [9–11]. In this study, TiN_x is deposited by titanium DC magnetron sputtering in an argon and nitrogen gas mixture. A lot of work has already been done in this field, but the industrial goal determines two original constraints: firstly, the substrate could not be heated too much to avoid structural change and secondly, to achieve a final 'in-line' steel coil-coating unit, the substrate must be connected to the earth potential.

It is well known that the most important parameters governing the physical properties of these films are the nitrogen partial pressure, the deposition temperature and the substrate bias voltage [12,13]. This study suggests modifying the deposition conditions of TiN_x in order to create a range of different coloured films dedicated to replacing current decorative coatings produced by wet technologies. In this paper, we investigate the influence of nitrogen mass flow ϕ_{N_2} on the titanium nitride physical properties in order to obtain precise colour control without heating and biasing tools. Results obtained by optical measurements are discussed in order to correlate the import of titanium nitride physical

* Corresponding author. Fax: +32-81725474.
E-mail address: philippe.roquiny@fundp.ac.be (P. Roquiny)

0257-8972/99/$ – see front matter
PII: S0257-8972(99)00076-6

properties such as stoichiometry and structure with the coating visual appearance.

2. Experimental procedure

2.1. Sample preparation

TiN_x coatings were produced by DC reactive magnetron sputtering. The vacuum chamber ($\cong 0.25\ m^3$) was equipped with a 63.5 cm^2 (90 mm diameter) magnetron cathode and a 1000 l/min turbo molecular pump. The base pressure was less than 5×10^{-4} Pa and the deposition working pressure and plasma current density were maintained respectively at 0.30 Pa and 8 mA/cm^2. In these conditions, the sample temperature measured with a thermocouple placed at the rear did not exceed 100°C onto grounded substrates placed at 55 mm from the sputtering target. The study of the deposition rate versus nitrogen partial pressure of the incoming gas mass flow is presented elsewhere [14]. So, thicknesses are easily calculated with these calibrated deposition rates multiplied by time.

Two types of substrate have been chosen to analyse the physical properties of the coating. For optical transmission spectra analysis, conventional microscope glass slides have been used, whereas for other characterisations, polished monocrystalline silicon wafers (100) have been coated. Both substrates were rinsed in acetone and plasma etched for approximately 10 min at 0.5 Pa in pure argon atmosphere prior to each nitride deposition.

2.2. Optical properties and colour

In order to avoid interface reflection interference and to study only the optical response of the film, transmission spectra have been scanned with wavelengths from 400 nm to 600 nm through various layer thicknesses deposited onto glass substrates. For further analysis, one nitride thickness has been chosen, therefore the coating appearance is only governed by the TiN_x layer and not by the substrate.

Colour and gloss, which are the most important properties of decorative coatings, were studied by spectral reflectance spectroscopy with a Micro Color tristimulus colorimeter equipped with an Ulbricht globe coupled to a xenon flash lamp for diffuse illumination of the sample. The light diffuse reflection from the sample was measured at an angle of 8°, in accordance with the German industrial standard DIN5033 [6,7,15,16]. Results are presented in both physiologically relevant CIE $L^*a^*b^*$ and physically linked x, y, Y colorimetric systems.

2.3. Composition and structure

The nitrogen content in the films was determined using the well-known $^{15}N(p,\alpha\gamma)^{12}C$ nuclear reaction. At a proton energy of 429 keV, a sharp and very intense resonance of this nuclear reaction occurs. An automatic energy scan system mounted on a Van De Graaff accelerator is used to obtain an excitation curve, and gives the nitrogen depth profile concentration compared to a standard sample [17–20].

To complete the composition analysis by resonant nuclear reaction (RNRA), Rutherford backscattering spectroscopy (RBS) at 140° with a 2.4 MeV ^4He beam was also performed on the sample. Conventional RBS simulation was computed with the RUMP program to extract the sample composition from the spectra [20,21]. The structure and crystalline parameters of some remarkable layers were also analysed by glancing angle X-ray diffraction of the Co Kα wavelength (1.7902 Å) selected on a Philips θ–2θ equipment [22].

3. Results

3.1. Transmission spectra

Fig. 1 shows the light transmission spectra $T(\lambda)$ through different film thicknesses from 50 nm to 600 nm for TiN_x coatings produced under a 4 sccm nitrogen mass flow. As can be seen from the figure, $T(\lambda)$ has already fallen under 3.8% with the 50 nm thick layer deposited onto glass substrate. This result shows that this thickness, which corresponds to a 100 nm light outward/return path, is already sufficient to avoid interference phenomena between light reflected from the film and light reflected from the substrate surface. To use the same thicknesses for samples in nuclear analysis, the

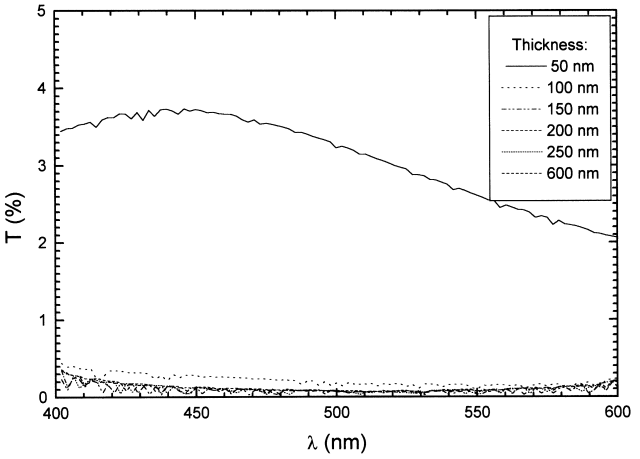

Fig. 1. Light transmission spectra $T(\lambda)$ from 400 to 600 nm through six different TiN_x film thicknesses deposited onto glass substrates (4 sccm N_2, 0.30 Pa, 8 mA/cm^2).

colorimetry determination has been carried out with 200 nm thick TiN_x coatings. It should also be noted for further discussion that maximum transmission occurs near $\lambda = 444$ nm through the 50 nm thick TiN_x layer.

3.2. Colorimetry

12 200 nm thick nitride films have been deposited on silicon substrate under ϕ_{N_2} ranging from 0 to 67 sccm for a 100 sccm total ($N_2 + Ar$) mass flow. Fig. 2 presents the chromatic diagram in the physiologically relevant a^* (green–red axis), b^* (blue–yellow) system for all these TiN_x coatings. Some interesting reference samples have also been picked out. On the figure, the data describe a loop curve in the a^*, b^* space as the nitrogen mass flow increases. Starting from the grey metallic appearance, the colour jumps to a gold-like yellow with very small ϕ_{N_2} increase: 0 to 2 sccm. Then, for further ϕ_{N_2} growth from 4 to 67 sccm, b^* decreases very slowly, i.e. the coating appearance is less yellow and finally becomes slowly more brown. The same conclusions are presented in the literature [6,7], where a loop curve with $a^* < 30$ and $b^* < 12$ is also observed as ϕ_{N_2} increases.

Fig. 3 shows the dependence of gloss (L^*) with ϕ_{N_2}. It can be seen that L^* falls from 75 to less than 65 with a 2 sccm N_2 increase. The further measurements are once more grouped together in the same range: L^* decreases less rapidly to reach 57 and becomes stable around this value. The coating appearance becomes brown and dark as the nitrogen content in the sputtering gas discharge increases.

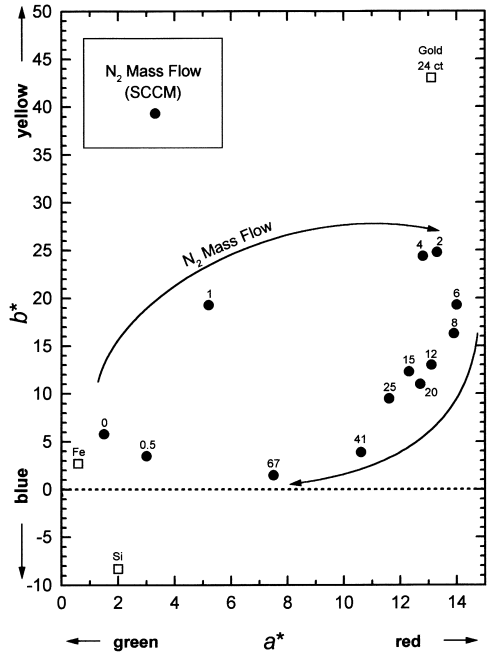

Fig. 2. Chromatic diagram in the physiologically relevant a^* (green–red axis), b^* (blue–yellow) system (CIE $L^*a^*b^*$) for TiN_x films deposited onto polished silicon substrates under ϕ_{N_2} between 0 and 67 sccm N_2 (0.30 Pa, 8 mA/cm^2). Each data is labelled with nitrogen mass flow used during the deposition. The arrows illustrate the loop curve evolution as ϕ_{N_2} increases. 24 carat gold, silicon and iron colour measurements are also picked as reference materials.

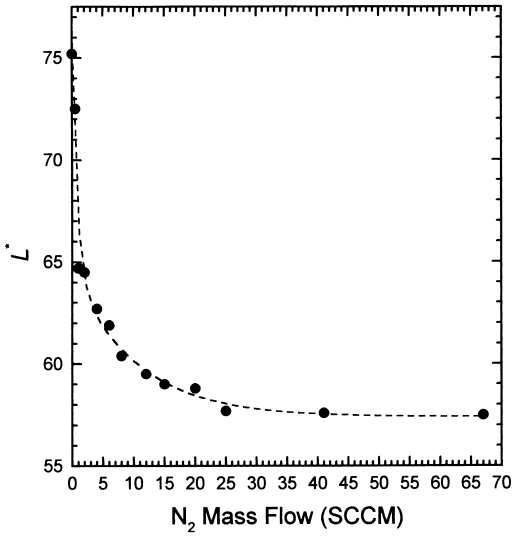

Fig. 3. Gloss L^* (CIE $L^*a^*b^*$) versus nitrogen mass flow used during TiN_x film deposition onto polished silicon substrates (0.30 Pa, 8 mA/cm^2).

The colour changes are difficult to interpret in this colorimetric system and, in order to discuss more physically these variations, the same measurements are also illustrated in the x, y colour space: a geometrical construction gives two meaningful physical parameters [16]. If a straight line is plotted between the data and the white coordinates (1/3,1/3), the intersections with the spectrum locus representing the pure colours give the main (λ_m) and the complementary (λ_c) wavelengths as shown in Fig. 4.

A loop curve evolution can be seen once again. As ϕ_{N_2} increases, λ_m growths and λ_c decreases (Fig. 4). Since λ_m represents the maximum value in the reflected light spectrum, it is not surprising that the main wavelengths of the more gold-like deposits produced under $\phi_{N_2} = 1$, 2 and 4 sccm surround the gold value (576 nm).

3.3. Composition and crystal structure

Fig. 5 shows Ti, N and O contents measured in the films by non-destructive nuclear reaction analysis (RNRA and RBS) versus ϕ_{N_2} in the sputtering discharge gas. It can be seen that the oxygen contamination is fairly constant around 2 at.% in almost all the layers while the Ti content decreases from 92 to 56 at.% and the N concentration increases from 2 to 41 at.% when ϕ_{N_2} goes from 0 to 2 sccm. Both contents also become fairly stable just below 50 at.% for further ϕ_{N_2} increase.

The samples produced under $\phi_{N_2} = 0$, 0.5, 2, 12 and 25 sccm have been analysed by glancing angle X-ray

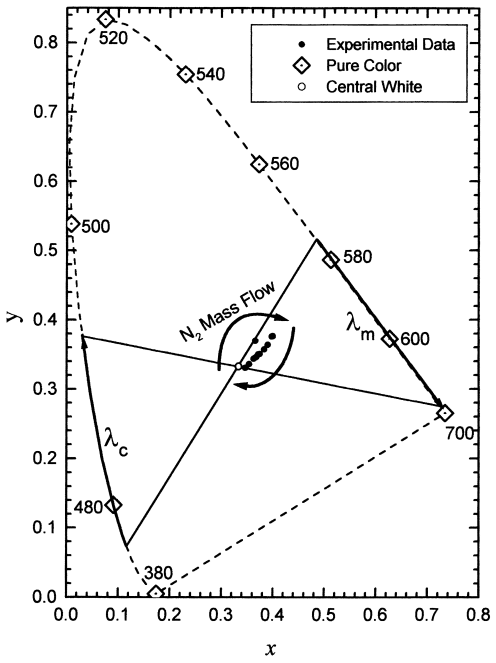

Fig. 4. Chromatic diagram in the physically relevant x, y system for TiN_x films deposited onto polished silicon substrates under different ϕ_{N_2} between 0 and 67 sccm N_2 (0.30 Pa, 8 mA/cm^2). The pure colours are labelled with their wavelengths expressed in nanometres on the spectrum locus while the white coordinates (1/3,1/3) are illustrated by an open circle. The straight line joining the data and the white centre gives two meaningful physical parameters. Intersection with the spectrum locus on the data side gives the main wavelength λ_m. Intersection on the other side gives the complementary wavelength λ_c. The arrows illustrate evolutions when ϕ_{N_2} increases.

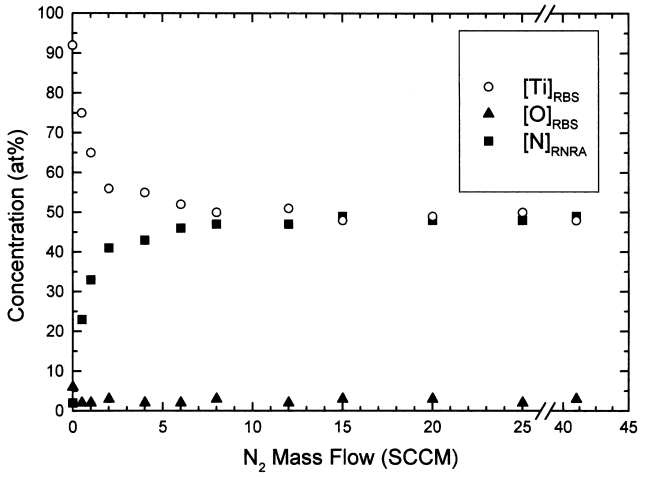

Fig. 5. Titanium, oxygen and nitrogen atomic concentration versus nitrogen mass flow used during TiN_x film deposition onto polished silicon substrates (0.30 Pa, 8 mA/cm^2). Nitrogen content was measured by $^{15}N(p,\alpha\gamma)^{12}C$ RNRA at 429 keV while titanium and oxygen were revealed by 2.4 MeV ^{4}He RBS at 175°.

diffraction. The layer deposited without N_2 in the gas sputtering discharge is the only one that exhibits the hexagonal compact structure of metallic titanium. All the other samples reveal the current face centred cubic

Table 1
Lattice parameter (a_0) and macroscopic stress (σ) computed with FCO (fixed crystal orientation) method [24] on GXRD spectra from TiN_x layers deposited under various ϕ_{N_2} (0.30 Pa, 8 mA/cm^2)

ϕ_{N_2} (sccm)	a_0 (nm)	σ (GPa)
0.5	0.42157	0.83
2	0.42419	−0.73
12	0.42521	−0.24
25	0.42507	−2.01

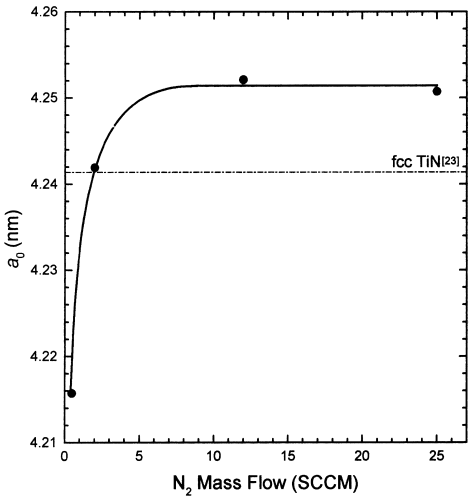

Fig. 6. TiN lattice parameter (a_0) computed with FCO (fixed crystal orientation) method [24] versus ϕ_{N_2} for layers deposited onto monocrystalline (100)-oriented silicon (0.30 Pa, 8 mA/cm^2).

titanium nitride phase [23]. Lattice parameter (a_0) and stress (σ) have been computed with the diffracted TiN peaks based on the FCO (fixed crystal orientation) method suggested by Quaeyhaegens et al. [24]. These results are listed in Table 1 and Fig. 6 shows the cubic lattice parameter a_0 evolution as ϕ_{N_2} increases for the four nitride layers mentioned above. It was subsequently found that a_0 is very beneath the stoichiometric value for $\phi_{N_2} = 0.5$ sccm where the coating colour is grey, but a_0 fairly matches this value for the gold-like film deposited under $\phi_{N_2} = 2$ sccm. The lattice parameters found for the other two brown layers built under important ϕ_{N_2} are very similar but just above the standard value. Macroscopic stresses are very reasonable, facing sometimes five times greater data measured by others authors for sputtered TiN_x. Unfortunately, further comparisons are difficult to perform because experiments from the literature are mainly carried out with a bias voltage applied on the substrate either/or at deposition temperature greater than 100°C [13,25,26].

4. Discussion

In view of the diffraction analysis, it seems likely that all the nitride layers deposited at low temperature with

N_2 in the gas discharge have grown with cubic crystal lattice, although the poor nitrogen content was measured for low ϕ_{N_2}. The TiN phase can be assumed to consist of a simple metal sublattice with nitrogen atoms occupying interstitial positions, thus forming a separate non-metal sublattice. The absence of nitrogen covalent bonding implies that titanium nitride possesses metallic properties [27].

Moreover, in their solar energy control material overview, Ribbing and Roos [10] explain that the transition metal nitrides are optically free electron-like due to their low intensity of interband transition at low photon energies. As for the noble metals, the optical properties can be mainly resolved in terms of the simple Drude theory in the IR and visible energy region. Then, on the basis of the Drude model, the unscreened plasma energy where the real part of the dielectric function $\epsilon_1(\omega)$ passes through zero can be used as a key value to relate the stoichiometry and crystal structure to the optical properties [28].

The unscreened plasma energy $\hbar\omega_p$ depends on the density of free electrons n and on an effective electron mass m^* since the unscreened plasma frequency ω_p is given by the expression $\sqrt{ne^2/\epsilon_0 m^*}$. The plasma frequency divides the visible spectrum into two parts: if $\omega > \omega_p$ and $\epsilon_1(\omega) > 0$ then the electromagnetic wave is propagated in the layer, on the contrary, if $\omega < \omega_p$ and $\epsilon_1(\omega) < 0$ then the light is reflected. This free electron-like behaviour must be completed with interband (bound carrier) absorption in the reflected electromagnetic wave energy range. For stoichiometric TiN, the interband transition occurs at the same energy as in gold, and the compound consequently exhibits a gold-like appearance [29].

On basis of Figs. 2 and 5, it can be seen that L^* shows the same evolution as the Ti content when ϕ_{N_2} increases. The number of free electrons n decreases with Ti concentration and the plasma energy moves towards lower energies. The reflected part of the light spectrum ($\omega < \omega_p$) is thus reduced, and that is why the gloss decreases. Unfortunately, the colorimetric data do not give direct measurement of $\epsilon_1(\omega)$ and then the plasma frequency is still unknown for the analysed samples. Nevertheless, we can suppose on the basis of the simple Drude theory that the complementary wavelength λ_c and thus the complementary photon energy E_c are characteristic of the spectral region where the nitride absorbs the light in the bulk. So, E_c could be assumed as a rough approximation of the plasma energy ($E_p = \hbar\omega_p$) where the electron gas is excited. Table 2 shows measured λ_c and computed E_c as a function of the N_2 mass flow used during the TiN_x deposition.

In the literature, the current estimation for E_p in TiN_x, where $x = 1$, was found to be 2.6 eV [28]. The mean value for our calculated E_c (2.55 eV) is very close to this standard E_p value. Moreover, Table 2 shows that E_c starts from 2.64 eV, decreases to around 2.56 eV between $\phi_{N_2} = 1$ and 6 sccm, becomes stable until $\phi_{N_2} = 25$ sccm and draws down again for $\phi_{N_2} = 41$ and 67 sccm. In view of Fig. 5, it is obvious that the first diminution of E_c can be correlated with the electron free density decrease due to the metallic nature reduction in the TiN lattice, i.e. the nitrogen content increases, while titanium concentration falls. For further ϕ_{N_2} supply, the Ti and N concentrations become constant just below 50 at.%. The consequence of the trend mentioned above is the E_c stabilisation around 2.55 eV. Unfortunately, the next lessening of this value cannot be explained in regard to the concentration analysis. However, that diminution could be attributed to an increase of crystal defects due, for example, to the non-negligible compressive stress measured in TiN_x layers deposited under high ϕ_{N_2} (see Table 1). These defects can affect strongly the electron density and then the amortised spectrum [10]. That is probably the reason why E_c is again reduced in these TiN_x layers but impossible to control with ϕ_{N_2}.

Table 2
Complementary wavelengths (λ_c) and associated photon energies (E_c) deduced from x, y chromaticity diagram for TiN_x layers deposited under various ϕ_{N_2} (0.30 Pa, 8 mA/cm^2)

ϕ_{N_2} (sccm)	λ_c (nm)	E_c (eV)
0	$\cong 700$	1.77
0.5	undefined	–
1	470	2.64
2	480	2.58
4	480	2.58
6	483	2.56
8	483	2.56
12	485	2.55
15	485	2.55
20	485	2.55
25	485	2.55
41	493	2.51
67	525	2.36

Furthermore, in TiN_x, the transmitted light maximum intensity occurs very near the reflected minimum [10]. That is why the photon energy (2.79 eV) revealed by the maximum transmitted intensity in Fig. 1 is likewise close to the standard $\hbar\omega_p$ value.

5. Conclusion

Colours from metallic grey to gold and finally brownish red have been obtained as the nitrogen mass flow is raised in the gas discharge. It was shown that these TiN_x layer colour variations can also be resolved in terms of the Drude model. As the titanium metallic nature of the compound decreases, the absorbed part of

the spectra moves towards lower energies. When the minimum titanium concentration in the deposited films is reached (N_2 mass flow >4 sccm), crystalline defects affect also the amortised spectra but are difficult to control. In conclusion, as the N_2 content in the gas discharge guides the nitrogen composition, it is the key parameter in colour control for TiN_x sputtered films, especially when N_2 mass flow is less than 4 sccm. Further research is in progress on nitrides deposited under low reactive gas mass flow.

Acknowledgements

This work is supported by the Ministère de la Région Wallonne (Belgium) within the FISRT Program (Programme de Formation et d'Impulsion à la Recherche Scientifique et Technologique) and by the Cockerill Sambre Research and Development Centre. The authors wish to thank Professor L. Stals and Professor C. Quaeyhaegens from the Institute for Materials Research of the Limburg's Universitair Centrum for the GXRD analyses and Ms. F. Frising from the Laboratoire de Didactique en Physique (Facultés Universitaires Notre-Dame de la Paix, Namur) for her help during the optical spectra measurement.

References

[1] D.J. Smukowski, Environmental regulation of surface engineering, in: C.M. Cotell, J.A. Sprague, F.A. Smith Jr. (Eds.), Surface Engineering, ASM Handbook Vol. 5, ASM International, Materials Park, OH, 1994, pp. 911–917.
[2] Commission of the European Communities, Proposal for a council directive establishing the framework for Community action in the field of water policy, Official Journal of the European Communities C series 184/97, Strasbourg, 1997, pp. 20–90.
[3] W.D. Sproul, J. Vac. Sci. Technol. A 12 (4) (1994) 1595.
[4] P.C. Jonshon, Metal Finish. April (1991) 61.
[5] H.A. Jehn, J.H. Kim, S. Hofmann, Surf. Coat. Technol. 36 (1988) 715.
[6] G. Reiners, H. Hantsche, H.A. Jehn, U. Kopacz, A. Rack, Surf. Coat. Technol. 54/55 (1992) 273.
[7] H.A. Jehn, Surface engineering in the Industrial practice: decorative coatings, in: Y. Pauleau (Ed.), Materials and Processes for Surface and Interface Engineering, Kluwer Academic, Dordrecht, 1995, pp. 359–370.
[8] Y. Miyamoto, Y. Kubo, N. Ono, M. Hashimoto, T. Takashi, I. Ito, F. Arezzo, P. Gimondo, Thin Solid Films 270 (1995) 253.
[9] H. Randhawa, Surf. Coat. Technol. 36 (1988) 829.
[10] C.G. Ribbing, A. Roos, SPIE Int. Symp. on Optical Thin Films V, San Diego, CA, 30 July–1 August, R.L. Hall (Ed.), Proc. SPIEE Vol. 3133, SPIE, Bellingham, WA, 1997, pp. 148–162.
[11] J.-E. Sundgren, Metastable hard coatings, in: Y. Pauleau, P.B. Barna (Eds.), Protective Coatings and Thin Films, Kluwer Academic, Dordrecht, 1997, pp. 335–344.
[12] W.D. Sproul, P.J. Rudnik, M.E. Graham, Surf. Coat. Technol. 39/40 (1989) 355–363.
[13] V. Valvoda, J. Alloys Comp. 219 (1995) 83.
[14] Ph. Roquiny, F. Bodart, S. Lucas, G. Terwagne, 11th Int. Colloq. on Plasma Processes, Le Mans, France, 25–29 May, A. Ricard (Ed.), CIP'97 Proceedings, CIP, Paris, 1997, pp. 28–32.
[15] ISO 7724/1,2,3, 1984.
[16] Y. Dordet, La colorimetrie, principes et applications, Eyrolles, Paris, 1990.
[17] B. Maurel, G. Amsel, Nucl. Instrum. Meth. 218 (1983) 159.
[18] G. Terwagne, M. Piette, F. Bodart, Nucl. Instrum. Meth. B 19/20 (1987) 145.
[19] G. Terwagne, S. Lucas, F. Bodart, Nucl. Instrum. Meth. B 66 (1992) 262.
[20] G. Deconninck, Introduction to Radioanalytical Physics, Elsevier–Akademia Kiado, Budapest, 1978, pp. 100–125.
[21] L.R. Doolittle, Nucl. Instrum. Meth. B 9 (1985) 344.
[22] C. Quaeyhaegens, M. Van Stappen, L.M. Stals, F. Bodart, G. Terwagne, R. Vlaeminck, Surf. Coat. Technol. 54/55 (1992) 279.
[23] JCPDS Powder Diffraction File, number 38-1420, International Centre for Diffraction Data, Swarthmore, 1995.
[24] C. Quaeyhaegens, G. Knuyt, L.M. Stals, J. Vac. Sci. Technol. A, submitted.
[25] A.J. Perry, A.F. Tian, J.R. Treglio, C. Loomis, Surf. Coat. Technol. 68/69 (1994) 528.
[26] B. Navinsek, P. Panjan, A. Cvelbar, Surf. Coat. Technol. 74/75 (1995) 155.
[27] N. Savvides, B. Widow, J. Appl. Phys. 64 (1988) 234.
[28] S. Logothedis, I. Alexendrou, J. Stoemenos, Appl. Surf. Sci. 86 (1995) 185.
[29] S. Logothedis, I. Alexendrou, A. Papadopoulos, J. Appl. Phys. 77 (1995) 1043.